JVSTB Journal of Vacuum Science & Technology B

Effect of fluoroalkyl substituents on the reactions of alkylchlorosilanes with mold surfaces for nanoimprint lithography

Jem-Kun Chen, Fu-Hsiang Ko, Kuen-Fong Hsieh, Cheng-Tung Chou, and Feng-Chih Chang

Citation: Journal of Vacuum Science & Technology B **22**, 3233 (2004); doi: 10.1116/1.1815305
View online: http://dx.doi.org/10.1116/1.1815305
View Table of Contents: http://scitation.aip.org/content/avs/journal/jvstb/22/6?ver=pdfcov
Published by the AVS: Science & Technology of Materials, Interfaces, and Processing

Articles you may be interested in
Sidewall-angle dependent mold filling of three-dimensional microcavities in thermal nanoimprint lithography
J. Vac. Sci. Technol. B **30**, 06FB09 (2012); 10.1116/1.4764096

Improved release strategy for UV nanoimprint lithography
J. Vac. Sci. Technol. B **25**, 2430 (2007); 10.1116/1.2806969

UV nanoimprint materials: Surface energies, residual layers, and imprint quality
J. Vac. Sci. Technol. B **25**, 785 (2007); 10.1116/1.2732742

Phosphonate self-assembled monolayers on aluminum surfaces
J. Chem. Phys. **124**, 174710 (2006); 10.1063/1.2186311

Micronanotribological study of perfluorosilane SAMs for antistiction and low wear
J. Vac. Sci. Technol. B **23**, 995 (2005); 10.1116/1.1913674

Re-register for Table of Content Alerts

Create a profile.
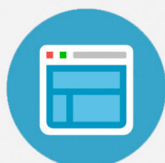
Sign up today!

Redistribution subject to AVS license or copyright; see http://scitation.aip.org/termsconditions. Download to IP: 140.113.38.11 On: Thu, 01 May 2014 04:08:55

Effect of fluoroalkyl substituents on the reactions of alkylchlorosilanes with mold surfaces for nanoimprint lithography

Jem-Kun Chen
Department of Applied Chemistry, National Chiao Tung University, Hsinchu, Taiwan

Fu-Hsiang Ko[a)]
National Nano Device Laboratories, and Institute of Nanotechnology, National Chiao Tung University, Hsinchu, Taiwan

Kuen-Fong Hsieh and Cheng-Tung Chou
Department of Chemical Engineering, National Central University, Taoyuan, Taiwan

Feng-Chih Chang[b)]
Department of Applied Chemistry, National Chiao Tung University, Hsinchu, Taiwan

(Received 2 June 2004; accepted 21 September 2004; published 10 December 2004)

We have applied trichloro(3,3,3-trifluoropropyl)silane (FPTS) and trichloro(1*H*,1*H*,2*H*,2*H*-perfluorooctyl)silane (FOTS) for the preparation of self-assembled film on a silicon mold for use as releasing, antisticking layers for nanoimprint lithography. From contact angle measurements, we have determined the surface energies of the molds in terms of their Lewis acid, Lewis base, and van der Waals components. The surface energies of the FPTS- and FOTS-derived film decreased as the annealing temperature and immersion time increased. Suitable self-assembled films were prepared by annealing at 150 °C for at least 1 h. The surface roughnesses of the self-assembled film formed from FPTS and FOTS were 0.468 and 0.189 nm, respectively. The lower surface energy and roughness of the FOTS-derived film on the silicon mold prevent both the adhesion and defect-formation problems from occurring during resist imprinting. The self-assembled films prepared on the mold are resistant to immersion in acid and base, but treatment with oxygen plasma has an adverse effect on these molds' stabilities. © *2004 American Vacuum Society.*
[DOI: 10.1116/1.1815305]

I. INTRODUCTION

The application of nanofabrication technologies to printing applications gives rise to the need to develop competitive parallel processes that may serve the technological demands of nanoelectronics and related areas. Thermal nanoimprint lithography is a promising method for fabricating integrated fine patterns using various materials.[1] In thermal nanoimprint lithography, a thermoplastic polymer is heated above its glass transition temperature (Tg), and a fine mold is pressed on the polymer. After cooling to below the value of Tg, the mold is released to reveal that the fine pattern on the mold has been transferred to the polymer. The use of thermal nanoimprinting processes has led to the fabrication of high-aspect-ratio patterns,[2] curved cross-sectional patterns,[3] and fine pattern transfers on novel plastic plates.[4]

One of the difficulties encountered in this process occurs during the release of the mold; often a critical defect is induced by the adhesion of the polymer to the mold. Stickiness is present during the process of mold release after thermal contact between mold and polymer. Strong adhesion is generally caused by capillary, electrostatic, and van der Waals forces and, in some cases, by hydrogen bonding. To overcome the adhesion problem, self-assembled films may be introduced. Self-assembled films, which are used widely to change the properties of surfaces, have important applications in surface science, molecular recognition, electrochemistry, microelectronic engineering, the preparation of nanotechnological structures and bioactive surfaces, and many other fields. In practice, one of the most commonly used self-assembled films is that of an organosilane monolayer on a hydroxyl-covered surface, such as silica, sapphire, or oxidized silicon. Various techniques[5–13] have been applied to

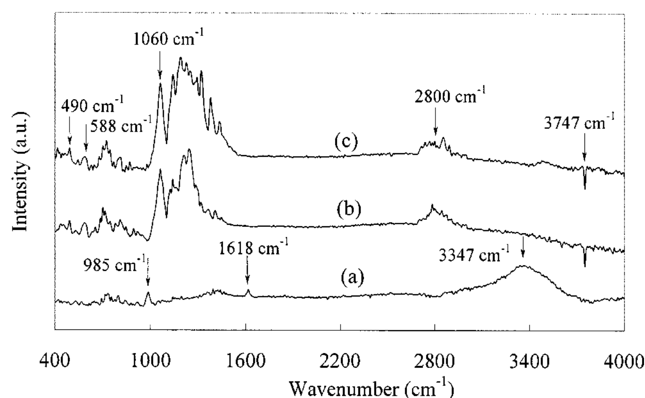

FIG. 1. FTIR spectra of the mold of (a) hydrated silica at room temperature, (b) the FOTS-derived self-assembled film annealed at 150 °C for 2 h, and (c) the FPTS-derived self-assembled film annealed at 150 °C for 2 h.

a)Author to whom correspondence should be addressed; electronic mail: fhko@ndl.gov.tw
b)Author to whom correspondence should be addressed; electronic mail: changfc@mail.nctu.edu.tw

Redistribution subject to AVS license or copyright; see http://scitation.aip.org/termsconditions. Download to IP: 140.113.38.11 On: Thu, 01 May 2014 04:08:55

characterize the surfaces of organosilane film, including contact angle measurements, ellipsometry, UV-Vis spectroscopy, FTIR spectroscopy, and ESCA at variable angles, as have a number of instruments, such as x-ray diffractometers, AFMs, and STMs. Even so, very little detail is known about the process of self-assembled film formation.

Treating the mold surface with a monolayer of a fluorinated polymer has been introduced to minimize the surface energy of the mold and to reduce charge trapping.[4,14] In this article, we describe our investigations of the self-assembled film formation process by FTIR spectroscopy and our calculations of the film' surface energies; we have also evaluated the effects that the annealing temperature and immersion time have on the surface energies. In addition, from contact angle measurements we have determined the surface energies in terms of the Lewis acid, Lewis base, and van der Waals components. We have also carefully studied the surface morphologies of the self-assembled films on the mold and their imprinting onto resists.

II. EXPERIMENT

A. Self-assembled film formation

Trichloro(3,3,3-trifluoropropyl)silane (FPTS, $Cl_3SiCH_2CH_2CF_3$) and trichloro(1*H*,1*H*,2*H*,2*H*-perfluorooctyl)silane [FOTS, $Cl_3Si(CH_2)_2(CF_2)_5CF_3$], which we used as precursors of the self-assembled films, were purchased from Aldrich. Layer formation was simplified using the following three steps (Scheme 1): (a) physical adsorption of a self-assembled monolayer (SAM) to the previously adsorbed water on the silicon substrate, (b) hydration of the chlorosilane groups, and (c) polymerization of the SAMs onto the surface. This method changes a previously hydrophilic surface into a hydrophobic one.[15–18] A silicon wafer having a hydroxyl-functionalized surface was immersed in either 1% FPTS or FOTS in toluene for 1 h before being rinsed (cleaned) with toluene. These samples were annealed at 150 °C for at least 1 h to perform the condensation process that produces the covalent siloxane (i.e., Si–O–Si) bonds (see scheme 1).

B. Analysis of the self-assembled film

A FTIR spectrometer (Bio-Rad, Model FTS-40, MA, USA) was used to evaluate the structural changes in the self-assembled films after their annealing at 150 °C for 2 h. The surface properties of the self-assembled films were examined by contact angle measurements. Measurements of the thicknesses for the films were performed using a SOPRA SE-5 ellipsometer (SOPRA, France).[19–21] The films prepared from FPTS and FOTS were estimated to have thicknesses of 11.4 and 18.9 Å, respectively. The advancing and receding contact angles were determined from water, ethylene glycol, and diiodomethane. The measurements were performed by increasing the drop volume and recording the angle with the aid of a contact angle goniometer (GH100, Kruss, Germany).

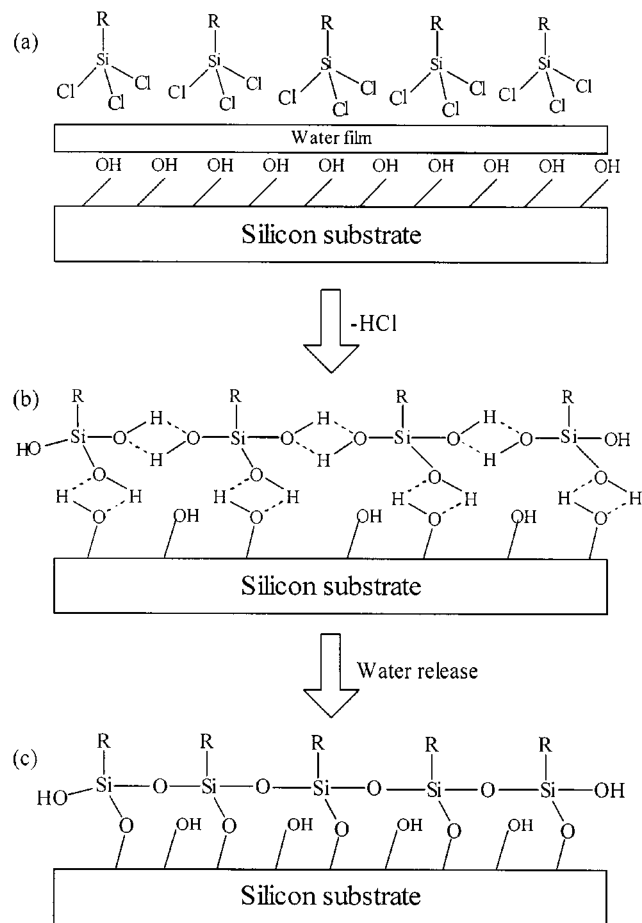

SCHEME 1.

The surface roughness and microscale profile were measured using an atomic force microscope (AFM, Digital Instruments, DI-5000, USA).

C. Surface energy calculation

Surface energies were evaluated using the Lifshitz–van der Waals acid/base theory (three-liquid acid/base method).[22,23] using the new "apolar" (Lifshitz–van der Waals, γ^{LW}) and "polar" (Lewis acid/base, γ^{AB}) concepts. Our theoretical approach follows the additive concept suggested by Fowkes[24]

$$\gamma = \gamma^{d} + \gamma^{AB}, \tag{1}$$

where γ^{d} stands for the dispersive term of the surface tension. The superscript *AB* refers to acid/base interaction. By regrouping the various components in Eq. (1), van Oss *et al.* expressed the surface energy as

$$\gamma = \gamma^{LW} + \gamma^{AB}. \tag{2}$$

In addition, two parameters have been created to describe the strength of the Lewis acid and base interactions:

γ^{+}=(Lewis) acid parameter of surface free energy;

γ^{-}=(Lewis) base parameter of surface free energy;

Redistribution subject to AVS license or copyright; see http://scitation.aip.org/termsconditions. Download to IP: 140.113.38.11 On: Thu, 01 May 2014 04:08:55

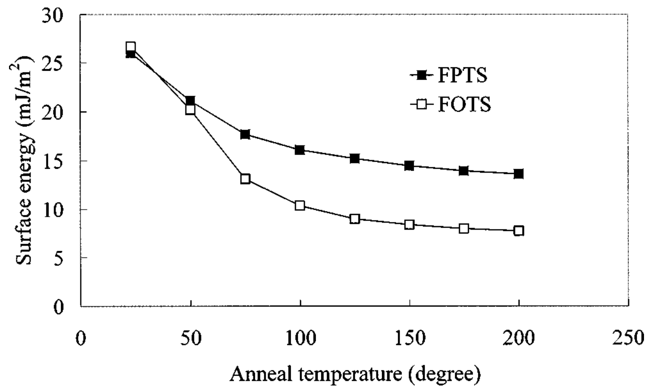

FIG. 2. Effect that the annealing temperature (°C) has on the surface energies of the molds incorporating self-assembled films formed from (a) FPTS and (b) FOTS.

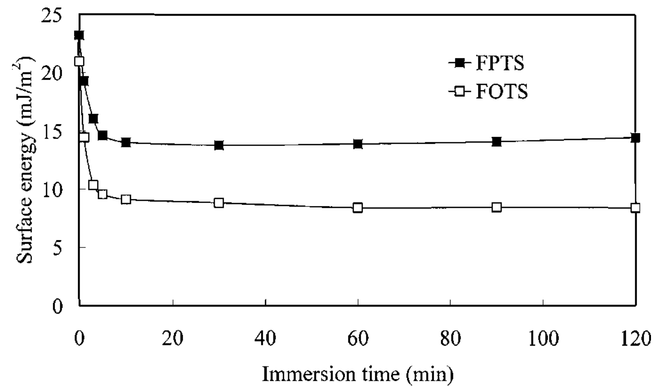

FIG. 3. Effects that the immersion times of the FPTS and FOTS solutions have on the surface energies of the molds modified with (a) FPTS- and (b) FOTS-derived self-assembled films.

$$\gamma^{AB} = 2(\gamma_s^{+}\gamma_s^{-})^{1/2}. \quad (3)$$

Van Oss, Good, and co-workers developed a "three-liquid procedure" [Eq. (4)] to determine γ_s by the contact angle technique:

$$\gamma_L(1+\cos\theta) = 2[(\gamma_s^{LW}\gamma_L^{LW})^{1/2} + (\gamma_s^{+}\gamma_L^{-})^{1/2} + (\gamma_s^{-}\gamma_L^{+})^{1/2}]. \quad (4)$$

To determine the surface free energy of a polymer solid requires two polar and one apolar solvent. The polar solvents usually used are water and ethylene glycol; the apolar liquid is either diiodomethane or R-bromonapthalene. The surface energy can be determined in terms of the LW, Lewis acid, and Lewis base parameters by solving these three equations [Eqs. (2)–(4)] simultaneously.[25–27]

D. Nanoimprinting using the molds with self-assembled films

Resists purchased from the SUMITOMO Chemical Company (22A4, Tokyo, Japan) were used for nanoimprinting. The success of combining the resist with the modified mold surface was demonstrated by using an imprint tool developed by Nanonex (Model NX-1000, US). The resists and mold were contacted at a preprint pressure of 200 psi and temperature of 110 °C; an imprint force of 380 psi was then used to press the mold into a 300-nm-thick resist over a duration of 5 min at 130 °C.

III. RESULTS AND DISCUSSION

A. Functional groups of self-assembled films

Figure 1 presents FTIR spectra reflecting the reactivity of FOTS and FPTS with the hydrated silica at room temperature, followed by annealing at 150 °C for 2 h. Hydrolyses of these silanes occurred by reaction with the surface water, as is evidenced by the disappearance of the H_2O deformation mode at 1618 cm^{-1}. The decreases in the intensities of the bands at both 3347 (SiO–H) and 978 cm^{-1} (Si–OH) are due to the formation of the FOTS- and FPTS-based films on the mold surface.[28] The surface assembled with FOTS [in Fig. 1(b)] and FPTS [in Fig. 1(c)] produce very weak bands at 588 and 490 cm^{-1} that represent the Si–Cl bonds.[29] The negative band at 3747 cm^{-1} is due to the SiO–H stretching mode of the isolated germinal surface silanols and its disappearance indicates that there is an interaction between the Si_sOH groups (Si_s refers to a surface silicon atom) and the alkylsilanol. A Si–O–Si bond can be formed by a reaction with the Si_s–OH groups, from cross-linking between adjacent alkylsilanols, or from the deposition of polymerization products on the surface. The key spectral region used to decipher the possible structures occurs at ≈1060 cm^{-1}; this region contains the Si–O–Si modes. The assignment is further complicated in the thin film studies because the bands in this region are superimposed over the intense bulk mode of silica. Subtle changes in the bulk Si–O–Si modes near the

TABLE I. Surface tension parameters calculated from the advancing contact angle for water, diiodomethane (DIM), and ethylene glycol (EG) on self-assembled films prepared from FPTS and FOTS at room temperature and at 150 °C.

Conditions	Contact angle of testing liquid (°)			Surface energy (mN/m)			
	Water	EG	DIM	γ_s^{LW}	γ_s^{-}	γ_s^{+}	γ_s
FOTS-derived film annealed at 23 °C	94.2	87.4	93.3	11.28	2.36	1.21	17.01
FOTS-derived film annealed at 150 °C	104.6	106.1	110.5	5.35	2.68	0.57	8.41
FPTS-derived film annealed at 23 °C	75.9	68.5	79	18.01	3.43	1.61	29.05
FPTS-derived film annealed at 150 °C	92.9	98.6	94.9	10.62	3.72	0.11	14.48

Redistribution subject to AVS license or copyright; see http://scitation.aip.org/termsconditions. Download to IP: 140.113.38.11 On: Thu, 01 May 2014 04:08:55

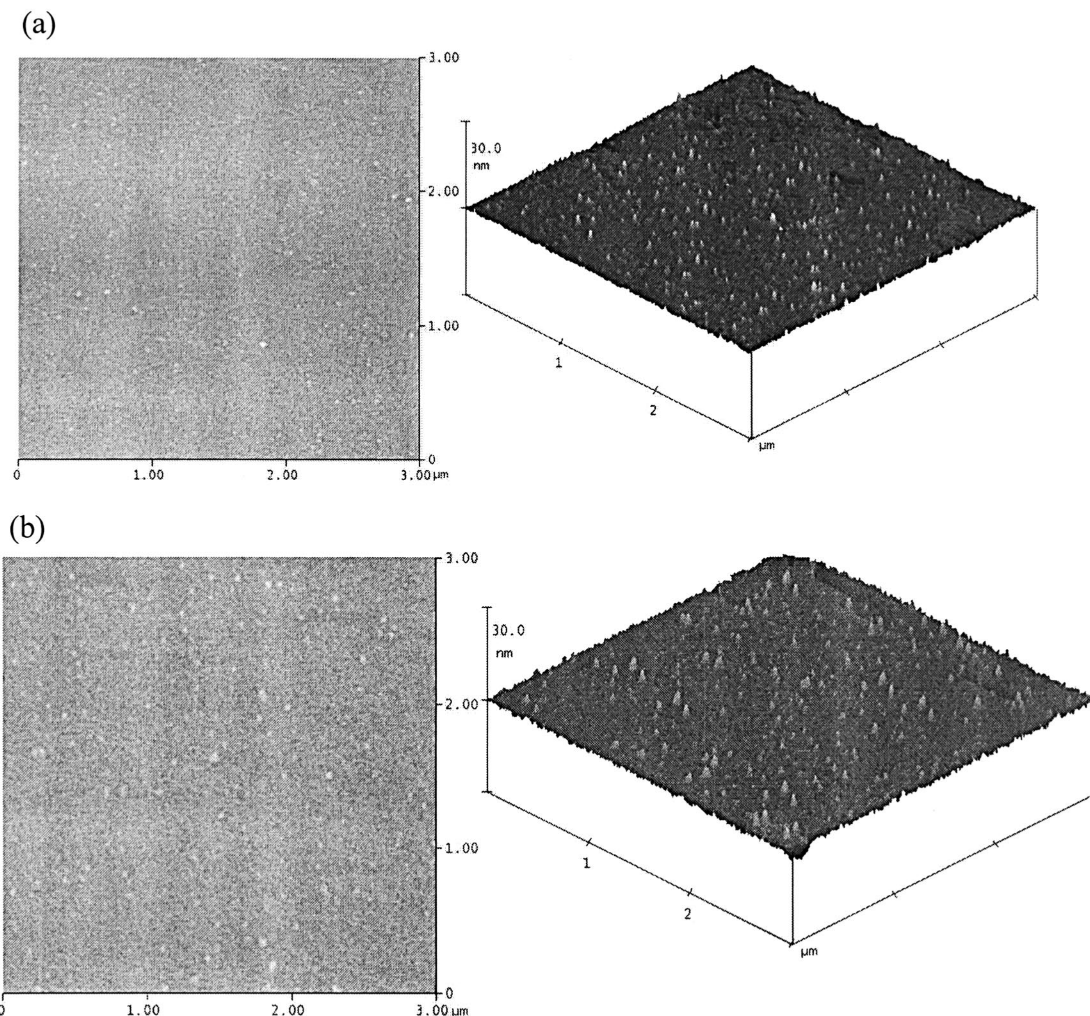

FIG. 4. AFM images (1 μm$\times$1 μm) of the (a) FPTS- and (b) FOTS-derived self-assembled films obtained after immersion for 20 min and then annealing at 150 °C.

adsorbed species could produce spectral changes in the 1200–1000 cm^{-1} region. We attribute other bands located at 2800 cm^{-1} and between 1450 and 700 cm^{-1} to various C–H and C–F modes.

B. Surface free energy of the mold

The effects that the annealing temperature (°C) and immersion time (min) of FPTS and FOTS have the surface energy are depicted in Figs. 2 and 3, respectively. Figure 2 clearly reveals that the surface energy decreases as the annealing temperature increases. This observation suggests that the reaction that occurs during self-assembled film formation is temperature-dependent and that high-temperature annealing is suitable for modification of the mold's surface. The FOTS-based film exhibits a lower surface energy than does the FPTS-derived one, and this finding may be attributable to the longer fluorocarbon chain of FOTS. Increasing the number of fluoride atoms is an effective means for reducing surface energy. We divide the curve in Fig. 2 into two regimes: a high-temperature region that displays a small surface energy variation, and a low-temperature region in which significant variations in surface energy occur. The crossover point between these two regimes is characterized by a well-defined temperature, T_{cw}, to which we assigned a value of 75±5 °C by fitting the data to a standard sigmoidal function[30–35] and selecting the intersection point of two tangents drawn to their respective regions. In the region below T_{cw}, the surface self-assembled films consist of loosely packed and disorganized assemblies of alkyl chains. In contrast, the surface self-assembled films are densely packed after annealing at temperatures above T_{cw}.

Prior to annealing at 150 °C, the mold required assembly of the FPTS or FOTS molecules on its surface. Figure 3 reveals clearly that the surface energies of the FPTS- and FOTS-derived films follow the same trend with respect to the immersion time. The surface energy quickly decreases up to an immersion time of 10 min, and then it remains level up to a time of 120 min. Consistent with the finding from Fig. 2, the FOTS-based films exhibit lower surface energies than the FPTS-derived ones. Table I suggests that the films that were

Redistribution subject to AVS license or copyright; see http://scitation.aip.org/termsconditions. Download to IP: 140.113.38.11 On: Thu, 01 May 2014 04:08:55

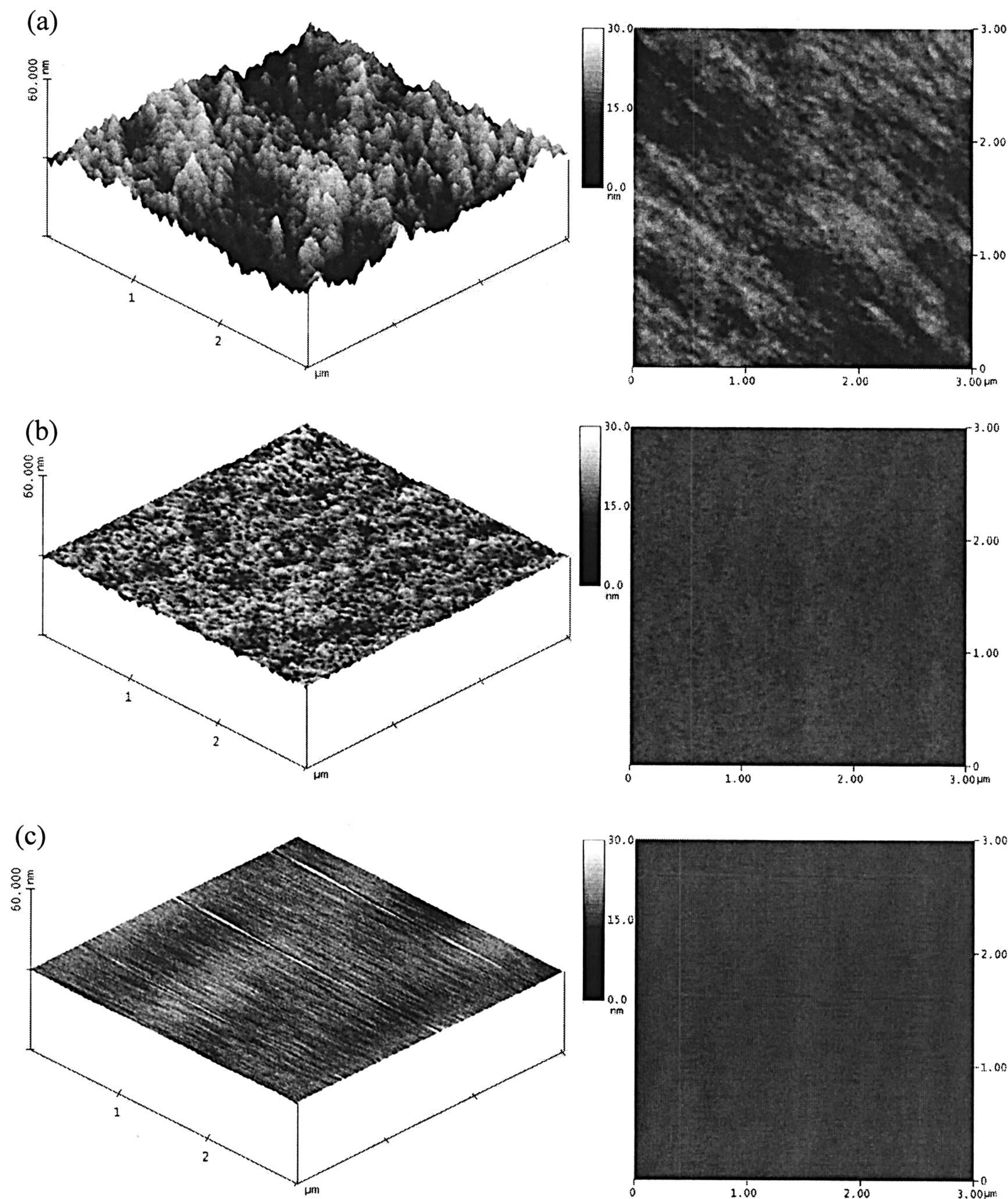

FIG. 5. AFM images (1 μm $\times$ 1 μm) of the resists after separation from the mold (a) in the absence of a self-assembled film, and in the presence of (b) FPTS- and (c) FOTS-derived self-assembled films.

annealed at room temperature (23 °C) have lower contact angles than those annealed at 150 °C. The Lewis base and acid components (γ^- and γ^+) of the surface energies, derived from the contact angle measurements, are also summarized in Table I. The Lewis acid component (γ^+) of the surface energy is close to zero after silanization at 150 °C, which leads to a vanishing value of the donor–acceptor component ($\gamma^{AB} \cong 0$). This observation suggests that the silanization upon annealing provides a surface that has a small affinity for base.[36] The acid/base terms (γ^{AB}) for silanes and silica oxide surface systems are small, and after the annealing process their total surface energies are contributed mainly by the γ^{LW} term.

C. Surface topography

Figure 4 displays AFM micrographs of the FPTS- and FOTS-derived films after annealing at a temperature of 150 °C. These AFM measurements indicate that the films for both self-assembled films were quite smooth. The root-mean-

Redistribution subject to AVS license or copyright; see http://scitation.aip.org/termsconditions. Download to IP: 140.113.38.11 On: Thu, 01 May 2014 04:08:55

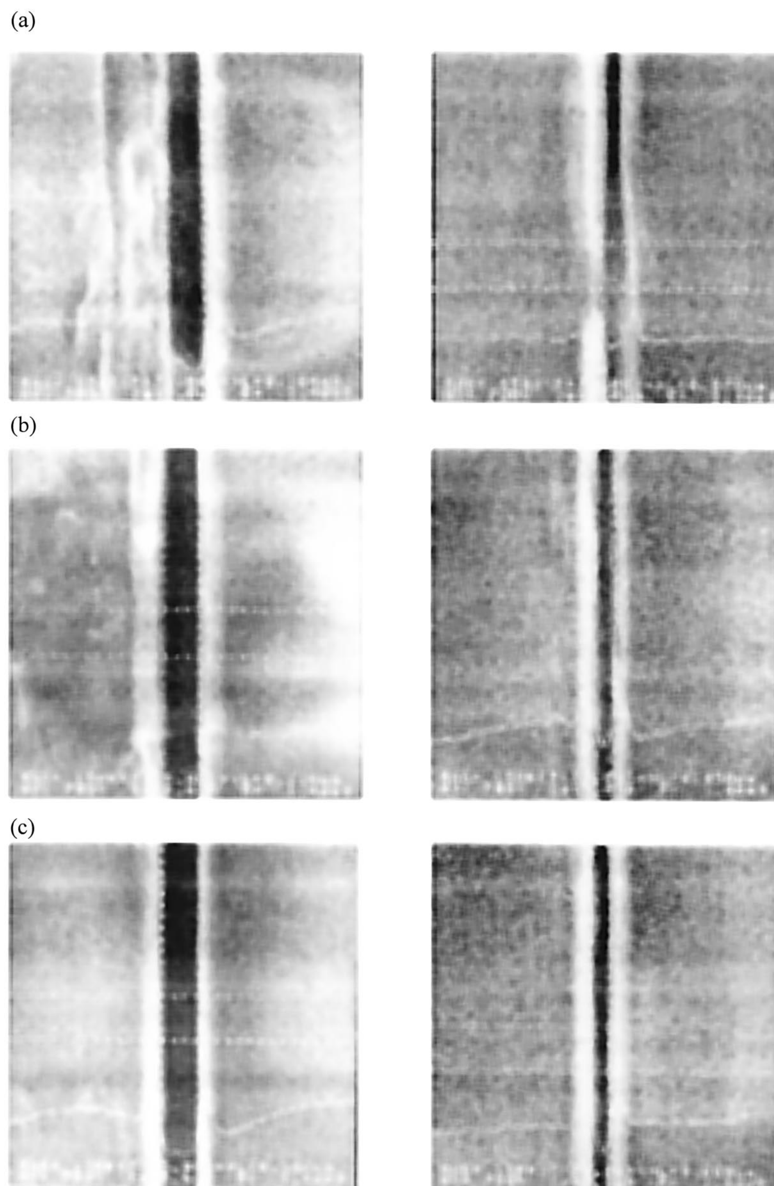

FIG. 6. SEM images of an isolated trench transferred by imprinting with lines of 120- and 60-nm thicknesses using (a) the mold in the absence of a self-assembled film, and in the presence of (b) FPTS- and (c) FOTS-derived self-assembled films.

square roughnesses of the films prepared from FPTS and FOTS were ≈0.468 and 0.189 nm, respectively. With FPTS, the AFM images display a larger number of bright spots that correspond to small patches in the film that are typically 10–15 Å thick and <40 Å in diameter.[37,38] We speculate that these patches are composed of densely packed silanes. The FPTS-derived film, which incorporates shorter fluorosiloxanes chains, exhibits a relatively larger number of these bright spots. Because the use of FOTS resulted in lower roughness and a lower number of bright spots in the mold, we believe that the surface of the FOTS-derived film, which has low surface energy, possesses fewer defects than the FPTS-based film.

In the nanoimprinting process, the transfer of a pattern from the mold to the resist on a substrate requires antiwetting of the surface of the mold to eliminate the defects induced by strain. Polymer contamination on the mold can be entrained in the polymerizing liquid, and the number of defects is reduced with repeated imprints.[39] Figure 5 displays AFM micrographs of the resist surface after separation from the mold in the absence of a self-assembled film [Fig. 5(a)] and in the presence of the FPTS- [Fig. 5(b)] and FOTS-derived self-assembled films [Fig. 5(c)]. The respective root-mean-square roughnesses of the resist surfaces are 1.568, 0.369, and 0.131 nm, respectively. The surface roughnesses of the resist films presented in Fig. 5 are derived from two mechanisms: physical adhesion and chemical adhesion.[40] Physical adhesion is due to weak interactions that occur at the interface (interface energy of ≈50 kJ/mol), such as van der Waals bonds or H bridges, which are effective over relatively long distances (0.2–0.5 nm). Chemical adhesion is caused by chemical bonds (ionic, atomic, or metal) that form between

Redistribution subject to AVS license or copyright; see http://scitation.aip.org/termsconditions. Download to IP: 140.113.38.11 On: Thu, 01 May 2014 04:08:55

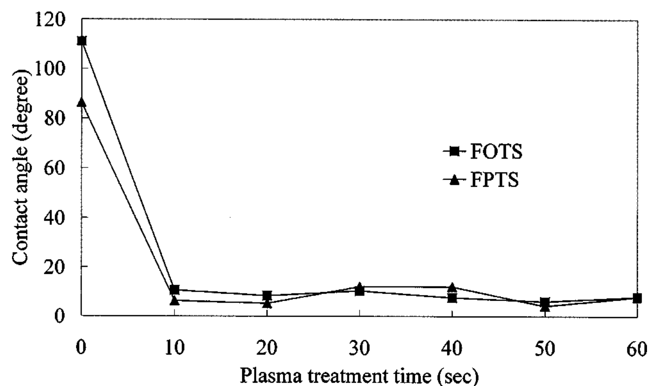

FIG. 7. Effect that the oxygen plasma treatment time has on the surface contact angle of the molds functionalized with FPTS- and FOTS-derived self-assembled films.

the surfaces (interfacial energies of 100–1000 kJ/mol); these bonds have shorter distances than do the physical interactions.

Figure 6 displays scanning electron micrograph (SEM) images of isolated trenches transferred by imprinting with lines of 120 and 60 nm thickness. Adhesion caused the flow of resists to form defects during the separation of the mold from the resists. Furthermore, the separation of the mold lacking a self-assembled film from the resist resulted in a shallow imprint pattern for the 60-nm-wide trench [Fig. 6(a)]. The number of defects caused by adhesion of the resist decreased when the separation was enacted using the molds functionalized with the FPTS- and FOTS-based self-assembled films [Figs. 6(b) and 6(c), respectively]. These results correlate well with the roughnesses of the molds that we observe in Fig. 5. The low surface energy of FOTS-based film decreases the adhesion, which resulting in a minimal number of defects.

D. Reliability of the FPTS- and FOTS-derived films

The stability of a mold after its modification with a self-assembled film is a very important parameter for ensuring the reliability of the imprinting process. We evaluated the molds' reliabilities by subjecting them the oxygen plasma treatment and immersion in acid and base solutions. Figure 7 presents the contact angles of the FPTS- and FOTS-derived self-assembled films after various plasma treatment times. Prior to treatment, the contact angles of water for these two self-assembled films were 86° and 111°, respectively, but the contact angles of water drop abruptly to ≈10° upon treatment with oxygen plasma; these value are even lower than that of bare silicon wafers prior to treatment. Therefore, it appears that oxygen plasma can decompose and oxide the FPTS- and FOTS-derived self-assembled films completely, which eliminates their antiwetting properties. In addition, we tested the acid and base resistances of these self-assembled films by immersing them in both 0.1 N HNO_3 and 0.1 N NaOH solutions at temperatures near 100 °C. Tables II and III list the results of the surface energy parameters calculated from the advancing contact angles for water, diiodomethane, and ethylene glycol. With respect to the acid resistance of the self-assembled films [Tables II(a) and III(a)], the Lewis acid component (γ^+) of the surface energy decreased as the immersion time increased, while the Lewis base component (γ^-) increased accordingly. The results suggest to the presence of nonbonded electron pairs on the FPTS- and FOTS-derived self-assembled films after their immersion in acid solutions; these electron pairs cause a change in the acid/base interactions (i.e., the values of γ^{AB}). In contrast, the dispersive component, γ^{LW}, is unaffected by acid immersion. The combination of these terms that affect the surface energy (i.e., γ^{LW}, γ^+, and γ^-) results in the total surface energies listed in Tables II(a) and III(a) remaining almost constant. This observation suggests that the FPTS-

TABLE II. Advancing contact angle and surface tension parameters for water, diiodomethane (DIM), and ethylene glycol (EG) on FPTS-derived self-assembled films after their immersion in 0.1 N (a) HNO_3 and (b) NaOH solutions at 100 °C as a function of immersion time.

	Contact angle for testing liquid (°)			Surface energy (mN/m)			
Immersion time (h)	Water	EG	DIM	γ_s^{LW}	γ_s^-	γ_s^+	γ_s
(a)							
0	92.9	98.6	94.9	11.46	2.36	0.64	14.4808
1	92.7	96.4	94.4	11.52	2.68	0.59	14.6824
2	93.2	91.3	93.1	11.32	3.43	0.51	14.8186
3	92.5	89.2	92.6	11.61	3.72	0.44	14.8836
(b)							
0	92.9	98.6	94.9	11.46	2.36	0.64	14.4808
1	92.7	99.9	94.6	11.55	2.11	0.72	14.5884
2	93.0	100.4	94.0	11.41	1.98	0.81	14.6176
3	93.1	101.0	93.6	11.38	1.82	0.89	14.6196

Redistribution subject to AVS license or copyright; see http://scitation.aip.org/termsconditions. Download to IP: 140.113.38.11 On: Thu, 01 May 2014 04:08:55

TABLE III. Advancing contact angle and surface tension parameters for water, diiodomethane (DIM), and ethylene glycol (EG) on FOTS-derived self-assembled films after their immersion in 0.1 N (a) HNO_3 and (b) NaOH solutions at 100 °C as a function of immersion time.

	Contact angles for testing liquid (°)			Surface energy (mN/m)			
Immersion time (h)	Water	EG	DIM	γ_s^{LW}	γ_s^-	γ_s^+	γ_s
(a)							
0	110.5	104.6	106.1	5.35	2.68	0.57	8.4052
1	110.1	102.2	105.2	5.47	2.98	0.54	8.6884
2	111.1	100.2	105.1	5.21	3.32	0.5	8.53
3	110.6	96.6	104.1	5.33	3.82	0.42	8.5388
(b)							
0	110.5	104.6	106.1	5.35	2.68	0.57	8.4052
1	110.9	105.5	106.1	5.26	2.54	0.62	8.4096
2	110.1	105.3	105.4	5.48	2.49	0.65	8.717
3	109.6	106.1	105.2	5.6	2.34	0.68	8.7824

and FOTS-derived self-assembled films have relatively high acid resistance. Similarly, the self-assembled film-functionalized molds are also resistant to alkali solutions, but the behavior of the Lewis acid (γ^+) and base (γ^-) components are quite different after the respective HNO_3 and NaOH immersions. NaOH immersion [Tables II(b) and III(b)] results in an increase in the Lewis acid component (γ^+) as the immersion time increases, but a corresponding decrease in the Lewis base component (γ^-). The summation of these two terms using Eq. (3) reveals that the acid/base term is not affected by the immersion time, which suggests a constant value of the donor–acceptor component. In addition, the dispersive component (γ^{LW}) also behaved in nearly the same manner. Hence, the total surface energies (γ_s) listed in Tables II(b) and III(b) suggest that the FPTS- and FOTS-derived self-assembled films have relatively high base resistance.

IV. CONCLUSIONS

We have successfully established the presence of chemical bonds between the FPTS- and FOTS-derived self-assembled films and the mold by analyzing FTIR spectra. The reaction that forms these self-assembled films is temperature-dependent and high-temperature annealing (150 °C) is suitable for modification of the silicon mold's surface. To identify the surface properties, we analyzed the surface energies on the molds' surfaces in terms of their Lewis base, Lewis acid, and van der Waals components. Modifying the mold with the FOTS-derived self-assembled film is a very effective means of ensuring that the mold's surface is free from defects during the imprinting process; this self-assembled film has the lowest surface energy. The self-assembled films prepared on the molds by using FPTS and FOTS are not resistant to treatment with oxygen plasma, but they are very resistant to acid and alkali solutions at 100 °C.

ACKNOWLEDGMENT

The authors thank the National Science Council of Taiwan for supporting this research financially through Contract No. NSC93-2113-M-492-003.

[1] S. Y. Chou, P. R. Krauss, and P. J. Renstrom, Appl. Phys. Lett. **67**, 3114 (1995).
[2] Y. Hirai, T. Yoshikawa, N. Takagi, S. Yoshida, and K. Yamamoto, J. Photopolym. Sci. Technol. **16**, 615 (2003).
[3] Y. Hirai, S. Harada, H. Kikuta, Y. Tanaka, M. Okano, S. Isaka, and M. Kobayasi, J. Vac. Sci. Technol. B **20**, 2867 (2003).
[4] Y. Hirai, N. Takagi, S. Harada, and Y. Tanaka, Sens. Micromach. Soc. **122**, 404 (2002).
[5] N. Tillman, A. Ulman, J. S. Schildkraut, and T. L. Penner, J. Am. Chem. Soc. **110**, 6136 (1998).
[6] A. N. Parikh, D. L. Allara, I. B. Azouz, and F. Rondelez, J. Phys. Chem. **98**, 7577 (1994).
[7] K. Mathauer and C. W. Frank, Langmuir **9**, 3446 (1993).
[8] J. D. Le Grange and J. L. Markham, Langmuir **9**, 1749 (1993).
[9] L. B. Hazell, I. S. Brown, and F. Freisinger, Surf. Interface Anal. **8**, 25 (1986).
[10] S. R. Wasserman, G. M. Whitesides, I. M. Tidswell, B. M. Ocko, P. S. Pershan, and J. D. Axe, J. Am. Chem. Soc. **111**, 5852 (1989).
[11] V. V. Tsukruk and D. H. Reneker, Polymer **36**, 1791 (1995).
[12] F. K. Perkins, E. A. Dobisz, S. L. Brandow, T. S. Koloski, J. M. Calvert, K. W. Rhee, J. E. Kosakowski, and C. R. K. Marrian, J. Vac. Sci. Technol. B **12**, 3725 (1994).
[13] J. L. Wilbur, H. A. Biebuyck, J. C. MacDonald, and G. M. Whitesides, Langmuir **11**, 825 (1995).
[14] H. Scheer, H. Schultz, T. Holffmann, and C. Torres, J. Vac. Sci. Technol. B **16**, 3917 (1998).
[15] P. Silberzan, L. Leger, D. Ausserre, and J. J. Benattar, Langmuir **7**, 1647 (1991).
[16] A. N. Parikh, D. L. Allara, I. B. Azouz, and F. Rondelez, J. Phys. Chem. **98**, 577 (1994).
[17] R. G. Good and C. J. van Oss, in *Modern Approaches to Wettability: Theory and Applications* (Plenum, New York, 1991), pp. 1–27.
[18] R. G. Good, M. K. Chaudhury, and C. J. van Oss, in *Fundamentals of Adhesion* (Plenum, New York, 1991), p. 153.
[19] P. Yeh, *Optical Waves in Layered Media* (Wiley–Interscience, New York, 1988).
[20] D. L. Allara and R. G. Nuzzo, Langmuir **1**, 52 (1987).
[21] S. R. Wasserman, G. M. Whitesides, I. M. Tidswell, B. M. Ocko, P. S. Pershan, and J. D. Axe, J. Am. Chem. Soc. **111**, 5852 (1989).

Redistribution subject to AVS license or copyright; see http://scitation.aip.org/termsconditions. Download to IP: 140.113.38.11 On: Thu, 01 May 2014 04:08:55

[22]C. J. Van Oss, M. K. Chaudhury, and R. J. Good, Chem. Rev. (Washington, D.C.) **88**, 927 (1988).
[23]C. J. Van Oss, L. Ju, M. K. Chaudhury, and R. J. Good, J. Colloid Interface Sci. **128**, 313 (1989).
[24]F. M. Fowkes, J. Phys. Chem. **66**, 382 (1962).
[25]G. W. C. Kaye and T. H. Laby, *Table of Physical and Chemical Constants*, 15th ed. (Longman Scientific and Technical, Harlow, 1992).
[26]*Handbook of Chemistry and Physics*, 76th ed., edited by D. R. Lide (CRC Press, Boca Raton, 1995).
[27]C. J. Drummond and D. Y. C. Chan, Langmuir **13**, 3890 (1997).
[28]C. P. Tripp and M. L. Hair, J. Phys. Chem. **97**, 5693 (1993).
[29]C. P. Tripp and M. L. Hair, Langmuir **7**, 923 (1991).
[30]A. Agresti, *Analysis of Ordinal Categorical Data* (Wiley–Interscience, New York, 1984).
[31]S. R. Wasserman, Y.-T. Tao, and G. M. Whitesides, Langmuir **5**, 1074 (1989).
[32]P. Silberzan, L. Leger, D. Aussere, and J. J. Benattar, Langmuir **7**, 1647 (1991).
[33]J. B. Brzoska, N. Shahidzadeh, and F. Rondelez, Nature (London) **360**, 719 (1992).
[34]R. J. Good, J. Am. Chem. Soc. **74**, 5041 (1952).
[35]J. F. Joanny and P. G. J. deGennes, Chem. Phys. **81**, 552 (1984).
[36]R. J. Good, in *Contact Angle, Wettability, and Adhesion* (VSP, Utrecht, The Netherlands, 1993).
[37]F. Fan, C. Maldarelli, and A. Couzis, Langmuir **19**, 3254 (2003).
[38]P. A. Heiney, K. Gru, and J. Fang, Langmuir **16**, 2651 (2000).
[39]T. Bailey, B. J. Choi, M. Colburn, M. Meissl, S. Shaya, J. G. Ekerdt, S. V. Sreenivasan, and C. G. Willson, J. Vac. Sci. Technol. B **18**, 3572 (2000).
[40]H. Weiss, Surf. Coat. Technol. **71**, 201 (1995).

Redistribution subject to AVS license or copyright; see http://scitation.aip.org/termsconditions. Download to IP: 140.113.38.11 On: Thu, 01 May 2014 04:08:55